Time-resolved spontaneous emission of excitons in a microcavity: Behavior of the individual exciton-photon mixed states

B. Sermage, S. Long, I. Abram, and J. Y. Marzin
FRANCE TELECOM, Centre National d'Etudes des Télécommunications, Paris B, Laboratoire de Bagneux, Boite Postale 107, 92225 Bagneux Cedex, France

J. Bloch, R. Planel, and V. Thierry-Mieg
Laboratoire de Microstructures et de Microélectronique, Centre National de la Recherche Scientifique, Boite Postale 107, 92225 Bagneux Cedex, France

(Received 1 May 1995; revised manuscript received 12 January 1996)

Low-temperature time-resolved luminescence experiments with 3-ps resolution have been performed on quantum-well excitons embedded in a nonguiding half-wave microcavity that displays the exciton-photon mode splitting. The spontaneous-emission dynamics of each of the two split components was studied as a function of the exciton-cavity detuning under resonant optical excitation. The spontaneous-emission decay rate is significantly modified with respect to the cavityless situation and its detuning dependence is accounted for by the strong radiative coupling between the radiant exciton states and the cavity photon modes. [S0163-1829(96)95024-9]

I. INTRODUCTION

The modification of the spontaneous-emission dynamics of semiconductors by their local dielectric environment has elicited a lot of interest in the past few years, in view of the possibility of obtaining thresholdless lasing or, equivalently, producing single-mode light-emitting diodes through the elimination of the energy losses associated with spontaneous emission.[1] In 1990 Yokoyama *et al.* showed that the spontaneous-emission lifetime of GaAs quantum-well excitons is shortened by a factor of 2 when the quantum well is embedded in a resonant microcavity.[2] This modification is generally understood by modeling the emitting species as a localized dipole inside the cavity: its lifetime is changed because of the modification of the free-space mode density by the cavity boundary conditions[3] or, equivalently, because of the electric field that is reflected by the cavity walls back onto the site of the emitting dipole.[4,5] The model of a localized dipole, however, cannot explain quantitatively the spontaneous-emission modification observed in Ref. 2. Indeed, the reflectivity of the Bragg mirrors that constitute the cavity drops to almost zero for angles of incidence inside the cavity larger than 20°, so that the change in the spontaneous-emission lifetime is at most of the order of 20%.

More recently, the observation of the exciton-photon mode splitting in the spectra of planar semiconductor microcavities containing few quantum wells[6–8] has led to the observation of quantum beats in the exciton emission, when the two components of the split line are pumped coherently.[9,10] At the same time, the observation of the splitting has brought forth the possibility of achieving a strong coupling between excitons and photons in the microcavity. This is analogous to what is observed in atomic cavity quantum electrodynamics (CQED) experiments[11] and thus may modify the spontaneous lifetime of the excitons.

In this paper, we report an experimental investigation on the modification of spontaneous-emission dynamics of quantum wells when they are embedded in a planar microcavity that displays an exciton-photon mode splitting of 4.8 meV. The experiments were performed at a temperature of 10 K and the sample was excited with a picosecond laser having a spectral width of about 0.4 meV so that it was possible to create particles separately in each coupled mode. Our results show that the emission rate of the quantum well embedded in a microcavity is significantly modified with respect to the cavityless situation. This modification is best accounted for by the strong electromagnetic coupling that is established between the extended exciton states and the modes of the microcavity.

The paper is organized as follows. In Sec II we describe the experiments and their results. In Sec. III we outline the main features of the exciton-photon strong-coupling model. In Sec. IV we analyze the experimental data in terms of the emission dynamics that arise in the strong-coupling model. Finally, in Sec. V we summarize our results and our conclusions.

II. EXPERIMENTS

Time-resolved luminescence measurements were performed on two molecular-beam epitaxy (MBE)-grown samples, each containing two 12-nm-thick strained $In_{0.14}Ga_{0.86}As$ quantum wells in a $\lambda/2$-thick AlAs spacer. In the first sample the AlAs spacer was sandwiched between two GaAs/AlAs Bragg mirrors made of 20 and 13.5 pairs and constituting a nonguiding $\lambda/2$ microcavity, as described in detail in Ref. 8. In order to be able to vary the cavity resonance without altering the other parameters, the sample was fabricated with a slight wedge, so that the effective thickness of the cavity L_c varies along the radial direction of the wafer by about 1.4% per mm, as determined by optical and x-ray measurements. The second sample had only one Bragg mirror (namely, the ''bottom'' mirror, closest to the substrate), while the ''top'' mirror was replaced by a 200-Å

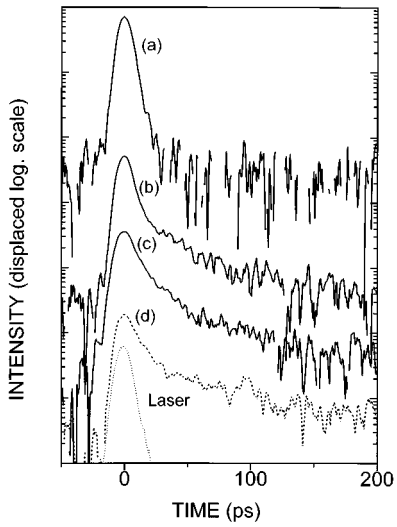

FIG. 1. Luminescence decay curves obtained with a laser excitation resonant with the lower state for different values of the detuning: (*a*) $\delta_0=E_{c0}-E_{x0}=-8.5$ meV, (*b*) $\delta_0=-1.5$, and (*c*) $\delta_0=3.5$ meV. The dashed curve (*d*) is the luminescence decay of the reference sample excited resonantly. The dotted curve (labeled ''Laser'') is the instrument response function.

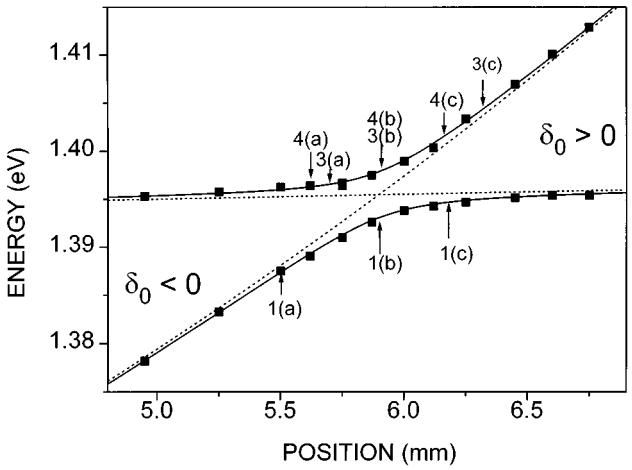

FIG. 2. Energies of the resonance luminescence signal, as a function of the position on the sample (■). The full line corresponds to the calculated energies of the coupled modes with a splitting $g=4.8$ meV and a wave vector in the plane $k_{\|}=9.6\times10^3$ cm^{-1}. The dotted curves are the uncoupled exciton and cavity energies for the same value of $k_{\|}$. The arrows show the positions where the decay curves of Figs. 1, 3 and 4 have been observed.

capping layer of GaAs to protect the AlAs spacer from oxidization. This second sample served as a reference in the measurement of the spontaneous-emission dynamics in the absence of a cavity.

The samples were maintained at a constant temperature of 10 K by means of a closed-cycle helium refrigerator and were excited by a mode-locked Ti-doped sapphire laser giving nearly Fourier-transform limited 1.5-ps-long pulses, at a repetition rate of 82 MHz. The laser beam was incident on the sample at an angle of about 8° and was focused to a spot of 50 μm diameter. The luminescence emerging with a maximum angle of about 11° was introduced in a 32-cm monochromator and was subsequently detected with a synchroscan streak camera (the sample was approximately perpendicular to the optical axis). The time resolution of the streak camera was limited mainly by the synchronization. Its transfer function was evaluated by recording directly the laser pulses: it corresponded to a Gaussian of 10 ps full width at half maximum so that its long-time tail falls to the $1/e$ value within about 3 ps, as can be seen from the steep slope of the wings of the laser pulse recording, in Fig. 1. The average power of the laser was kept between 1 and 100 μW (corresponding to between 0.01 and 1 W peak power).

When the excitation wavelength was scanned in the vicinity of the exciton energy ($E_{x0}=1.395$ eV), a strong resonance-enhanced signal of the luminescence intensity was observed for two distinct energies, corresponding to the two mixed exciton-photon states. A plot of the energies of the two states as a function of the position of the excitation spot on the sample (which corresponds essentially to a 1.4% variation of the cavity thickness per mm of displacement) is given in Fig. 2. The mirror-to-mirror separation could not be measured independently at 10 K but was deduced from the optical data to be approximately 145 nm at the exciton-cavity resonance. The curve on Fig. 2 is similar to that reported in Ref. 8 for the reflectivity and luminescence of the same sample at 77 K, except that here, in performing the fit we have taken into account the parabolic variation of the cavity thickness produced by the MBE-growth process and a slight linear variation of the quantum-well thickness. This gives an exciton energy $E_{x0}=1.3955$ eV and an exciton-photon mode splitting $g=4.8$ meV. The strong coupling between the cavity modes and the exciton is clearly at the origin of the strong resonance luminescence signal.

Time-resolved luminescence curves were obtained on different points of the sample (corresponding to different detunings $\delta_0=E_{c0}-E_{x0}$ between the exciton energy and the main cavity mode energy E_{c0}) for resonant excitation, in which the incident beam is tuned to the lower or to the upper state and emission is monitored at the same wavelength. When the excitation is resonant with the upper state, we also observe a resonance of the luminescence intensity coming from the lower states.

Figures 1 and 3 present some typical time-resolved luminescence curves for excitation resonant with the lower and the upper states of the microcavity sample at different cavity detunings as well as for the reference (cavityless) sample under resonant excitation. Figure 4 shows the time-resolved luminescence curves of the lower states when the excitation is resonant with the upper states. Two components may be distinguished in the curves of Figs. 1 and 3: a short and intense signal whose decay time (τ_1) varies between 3.5 ps (close to the resolution of the streak camera) and 17 ps and a second longer-lived component whose decay time (τ_2) is about 300–400 ps (the luminescence of the lower states, when the excitation is resonant with the upper state presents only the long decay). At first sight, we can distinguish two kind of decay curves in Figs. 1 and 3. The first kind corresponds either to the upper branch for $\delta_0=E_{c0}-E_{x0}>0$ or to the lower branch for $\delta_0<0$. In these decay curves, the first decay is very fast and the second component is too weak to be observed. The second kind corresponds to the upper branch for $\delta_0<0$ and the lower branch for $\delta_0>0$. In this case,

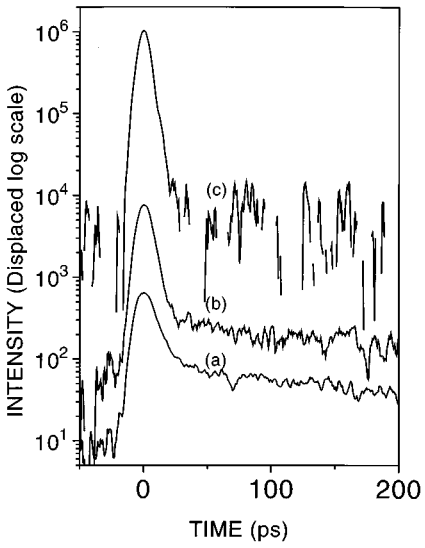

FIG. 3. Luminescence decay curves obtained with a laser excitation resonant with the upper states for different values of the detuning: (*a*) $\delta_0=E_{c0}-E_{x0}=-4.8$ meV, (*b*) $\delta_0=-1$ meV, and (*c*) $\delta_0=4.7$ meV.

the bi-exponential decay is very similar to the resonant luminescence of excitons in uncapped GaAs wells[12,13] (also observed in our cavityless reference sample in Fig. 1, with $\tau_1=14.5$ ps) and may be understood by invoking the distinction between the radiant and nonradiant exciton states. The former states correspond to the exciton states that can couple to light and consist of the excitons with angular momentum $J=1$ and with in-plane wave vectors $k_\parallel$ that are shorter than the photon wave vector $k_\parallel<k_0=nE_{x0}/\hbar c$ (n is the refractive index). The latter, which consist of the $J=1$ excitons with wave vector larger than the wave vector of light at the same frequency ($k_\parallel>k_0$) as well as of the $J=2$ excitons, cannot couple to the electromagnetic field and constitute a reservoir.

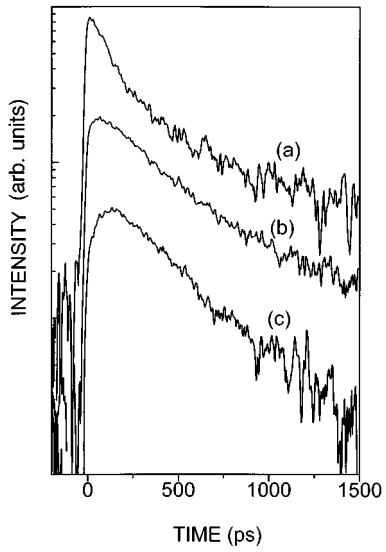

FIG. 4. Lower-state luminescence decay curves obtained with a laser excitation resonant with the upper states for different values of the detuning: (*a*) $\delta_0=-6.5$ meV, (*b*) $\delta_0=-1.5$ meV, and (*c*) $\delta_0=3.5$ meV.

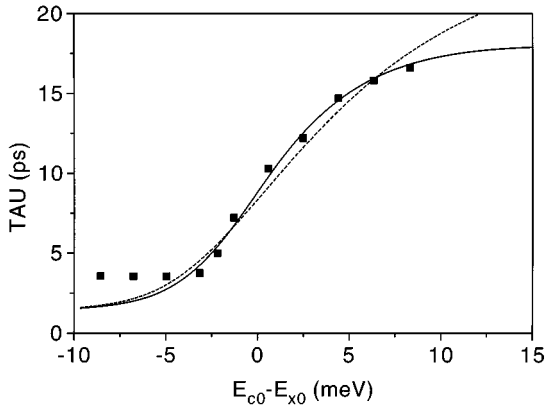

FIG. 5. Initial luminescence decay time under resonant excitation as a function of the exciton-cavity detuning $\delta_0=E_{c0}-E_{x0}$ (■). The data have not been corrected for the resolution of the streak camera (~3 ps). The dashed line is the lifetime calculated by the two-level model with $\tau_c=1.3$ ps, $\tau_x=26$ ps, and $k_\parallel=1.9\times10^4$ cm^{-1}. The full line is calculated using the polariton model with $\tau_{a0}=15.6$ ps, $\tau_c=1.3$ ps, and $k_\parallel=1.9\times10^4$ cm^{-1}.

The excitation pulse creates excitons in the radiant states at $t=0$, which subsequently can either recombine radiatively or interact with acoustic phonons and scatter to the nonradiant reservoir, thus giving rise to the fast initial decay. At later times, the excitons scatter back from the reservoir to the radiant states and then emit light, giving rise to the second, longer-lived, component.

Figure 5 presents a plot of the initial decay time τ_1 as a function of the exciton-cavity detuning δ_0 for the excitation resonant with the lower states. Finally, in Fig. 6 we present the initial instantaneous intensity of the resonant luminescence measured as a function of the exciton-cavity detuning.

III. THE EXCITON-PHOTON STRONG-COUPLING MODEL

The strong coupling between excitons and cavity modes can be described either in the framework of the polariton or

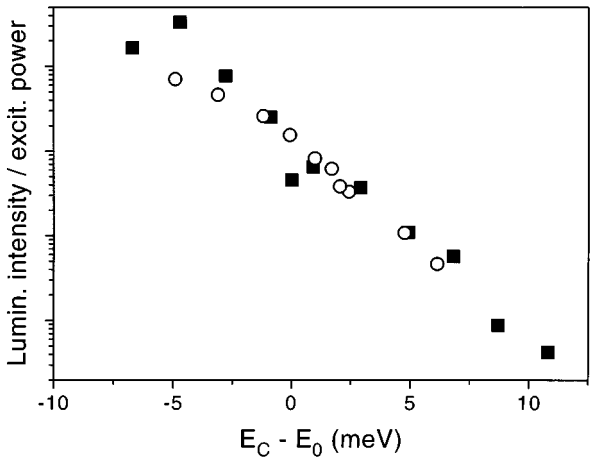

FIG. 6. Variaton of the ratio between the luminescence intensity I_L and the excitation power P_{ex} with the detuning $\delta_0=E_{c0}-E_{x0}$ (■). The open circles are the ratio of the measured $1-R$ value by the calculated τ_{rz}. The absolute values have no meaning. The two curves have been drawn close to one another to show that they have the same variation.

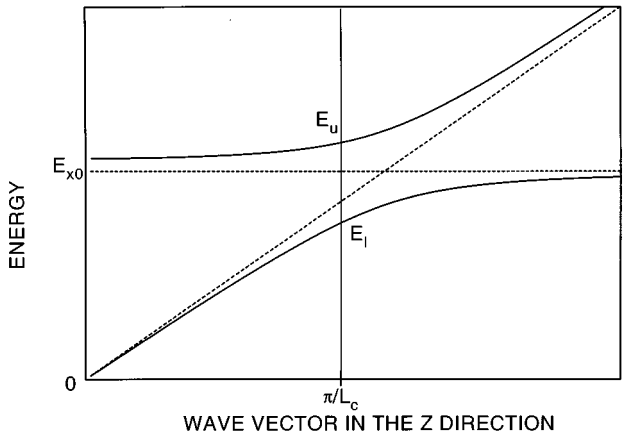

FIG. 7. Polariton dispersion curves in the z direction in the intracavity medium for $k_{\parallel}=0$. The energies of the upper and the lower states of the microcavity are the intersection of the polariton curves with the straight line $k_z=\pi/L_c$. The oscillator strength has been unrealistically increased to help the understanding of the figure.

with the more usual quantum-mechanic two-level model. Since these two descriptions are useful for the understanding of the lifetime of the coupled modes, we present in the following these two models.

A. The polariton model

The interest of this model[14–16] is that it relates the splitting of the coupled modes to known parameters of semiconductor physics. The propagation of polaritons in the z direction (perpendicular to the plane of the microcavity) is *a priori* better suited for bulk microcavities. However, it can also be used for quantum well microcavities provided that the exciton mass in the z direction is taken to be infinite and that one multiplies the oscillator strength of the excitons in the quantum wells by an adequate confinement factor. Another difference with the bulk case is that there is no additional boundary condition at the interfaces with the mirrors. In the following, we will limit our discussion to the case of a single exciton mode, associated with the E_1HH_1 $1s$ transition, with energy $E_{xk}=E_{x0}+\hbar^2k_{\parallel}^2/2M$, where M is the exciton translation mass, and with a $\lambda/2$ cavity with a single photon mode, with energy $E_{ck}=(\hbar c/n)\sqrt{k_z^2+k_{\parallel}^2}$. We replace the intracavity structure by an equivalent homogeneous material having the same oscillator strength and whose refractive index is the average of the refractive indices of the different layers. In this material, the dispersion of a polariton with wave vector $k=(k_z,k_{\parallel})$ and an energy E is given by the usual Hopfield model.[17,18]

$$\frac{\hbar^2c^2(k_z^2+k_{\parallel}^2)}{E^2}=\varepsilon_{\infty}+\frac{4\pi\beta E_{xk}^2}{E_{xk}^2-E^2}, \tag{1}$$

where the damping term $iE_{xk}\gamma$ is neglected and $4\pi\beta=\varepsilon_0-\varepsilon_{\infty}$ is the volumic oscillator strength of the excitons in the intracavity material (ε_0 and ε_{∞} are the dielectric constants below and above the exciton energy). The polariton dispersion curve for $k_{\parallel}=0$ is schematically shown in Fig. 7, where the exciton dispersion curve is flat because the excitons cannot move in the z direction. The oscillator strength $4\pi\beta$ is related to the volumic oscillator strength of the excitons in the well $4\pi\beta_{\mathrm{QW}}$.

$$4\pi\beta=4\pi\beta_{\mathrm{Qw}}\Gamma, \tag{2}$$

where Γ is the confinement factor of the quantum wells in the cavity for the confined mode of interest, i.e., the overlap between the wells and the square of the optical field. When the wells are situated at the antinode of the field, we can write

$$\Gamma\approx\frac{2N_Wd}{m_{\mathrm{eff}}L_c}, \tag{3}$$

where N_W is the number of wells, d is their thickness, and m_{eff} is the effective order of the cavity which takes into account the penetration of the electromagnetic field into the mirrors.[19]

The cavity confinement imposes $k_z=\pi/L_c$. This gives two modes (Fig. 7), referred to as upper and lower, whose energies E_u and E_1 are given by

$$E_{uJ}^2=\frac{E_{xk}^2+E_{ck}^2+g^2\pm\sqrt{(E_{xk}^2+E_{ck}^2+g^2)^2-4E_{xk}^2E_{ck}^2}}{2}, \tag{4}$$

where $g=\sqrt{4\pi\beta E_{x0}^2/\varepsilon_{\infty}}$ is the splitting between the modes at resonance.

In the vicinity of resonance, that is to say, when $E_{ck}\sim E_{xk}$, the energies of the two modes can be simplifies as

$$E_{u,l}=\frac{E_{xk}+E_{ck}}{2}\pm\frac{\sqrt{(E_{ck}-E_{xk})^2+g^2}}{2}. \tag{5}$$

It is worth noting that this expression of strong coupling is obtained in the framework of a linear-response theory, as pointed out by Zhu *et al.* in the case of atomic physics.[20]

These modes have been designated as cavity polaritons,[21] their dispersion curves as a function of $k_{\parallel}$ have been plotted in Fig. 8 for three representative values of the detuning $\delta_0=E_{c0}-E_{x0}$. Let us note that for the in-plane wave vectors larger than the limit of the stop band of the mirrors (k_{SB}), the dispersion curve should be exactly the exciton parabola (which is not the case in the figure).

B. The two-level model

The two-level model touches on the ideas of CQED, developed in the framework of atomic physics. The two subsystems sharing a single excitation quantum are designated by the state vectors $|X\rangle$ and $|C\rangle$ and correspond respectively to the exciton and cavity modes, which have the same wave vector in the plane ($k_{\parallel}$). They are coupled to each other by the radiative interaction. By invoking the rotating-wave approximation, the corresponding Hamiltonian can be written as

$$H=\frac{1}{2}\begin{pmatrix}\delta_k & g\\ g & -\delta_k\end{pmatrix}, \tag{6}$$

where $\delta_k=E_{ck}-E_{xk}$ and the origin of energies is taken at $(E_{xk}+E_{ck})/2$.

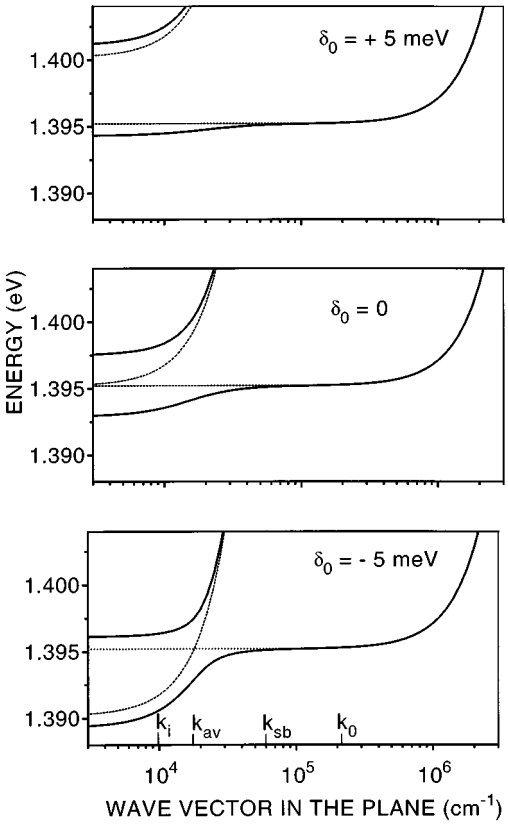

FIG. 8. Dispersion curves of the upper and the lower cavity polariton modes as a function of the wave vector in the plane for three values of the detuning. The dashed lines are the dispersion curves of the cavity without exciton and of the exciton without cavity. The parameters are those of the sample.

The eigenstates of this Hamiltonian are two exciton-photon mixed states, upper and lower modes, which can be represented as

$$|U\rangle = \frac{g}{\sqrt{2\Delta_k(\delta_k+\Delta_k)}}\,|X\rangle + \sqrt{\frac{\delta_k+\Delta_k}{2\Delta_k}}\,|C\rangle, \qquad (7a)$$

$$|L\rangle = \left(\frac{\delta_k+\Delta_k}{2\Delta_k}\right)^{1/2}|X\rangle - \frac{g}{\sqrt{2\Delta_k(\delta_k+\Delta_k)}}\,|C\rangle. \qquad (7b)$$

They lie at energies $(E_{xk}+E_{ck})/2 \pm \Delta_k/2$, with $\Delta_k = \sqrt{\delta_k^2+g^2}$, which is equivalent to Eq. (5). The two models give then the same results and are essentially equivalent. They differ only by the order of introduction of the different interactions: photon-exciton-cavity limit. The interest of the second model is that it gives directly the exciton and photon part of the mixed particles.

Equation (4) or (5) has been used to fit the experimental energies of the upper and lower states as thickness is varied. The energies of the coupled modes depend on g, δ_0, and $k_\parallel$. Since the incident angle is 8°, the component of the incident wave vector in the plane k_i is equal to 9.6×10^3 cm^{-1}. The fit presented in Fig. 2 has been obtained using this value for $k_\parallel$, $n=3.07$, $M=0.2m_0$, $g=4.8$ meV, a parabolic variation of the cavity thickness, and the same variation for the well thickness. Let us note that a modification of $k_\parallel$ changes the relation between the position on the sample and the detuning δ_0, but not the shape of the curve. The value of the splitting (4.8 meV) corresponds to $4\pi\beta = 1.11\times10^{-4}$. The effective order of the cavity is calculated as in Ref. 19, taking for the low-temperature refractive index of AlAs and GaAs the values $n_1=2.96$ (Ref. 22) and $n_2=3.517$.[23] We obtain $m_{\rm eff}=6.3$ and the modal overlap $\Gamma=0.0526$. The volumic oscillator strength of the excitons in the wells is then $4\pi\beta_{\rm QW}=2.12\times10^{-3}$. This value is very close to what can be calculated from the exciton binding energy in an $In_xGa_{1-x}As$ quantum well.[24,25] It is worth pointing out that the longitudinal transverse splitting $\Delta_{\rm LT}=2\pi\beta E_{x0}/\epsilon_\infty$ for the equivalent intracavity material is equal to 7.8 μeV, which is nearly three orders of magnitude smaller than the splitting between the lower and upper states. When divided by the confinement factor, it would be 149 μeV, which is larger than the known value for GaAs: 80 μeV,[26,27] because of the increase of the excitonic oscillator strength in quantum wells.

IV. DYNAMICS OF THE EXCITON-PHOTON MIXED STATES

The mixing of the radiant states of the exciton with the cavity modes, modifies the dynamics of the exciton luminescence inside the cavity. We will study the lifetime of the mixed modes in the framework of the two previous models.

A. The two-level model

Within the two-level model, the observed decay rate of each one of the mixed states is a linear combination of the exciton decay rate and the cavity decay rate. Thus the decay times of the upper (τ_U) and lower (τ_L) states are given respectively by

$$\frac{1}{\tau_U} = \frac{g^2}{2\Delta_k(\delta_k+\Delta_k)}\,\frac{1}{\tau_X} + \left(\frac{\delta_k+\Delta_k}{2\Delta_k}\right)\frac{1}{\tau_C} \qquad (8)$$

and

$$\frac{1}{\tau_L} = \left(\frac{\delta_k+\Delta_k}{2\Delta_k}\right)\frac{1}{\tau_X} + \frac{g^2}{2\Delta_k(\delta_k+\Delta_k)}\,\frac{1}{\tau_C}, \qquad (9)$$

where τ_X is the decay time for the exciton population, while τ_C is the decay time for the energy of the radiation field in the empty cavity (for example, through the emergence of a light beam in the z direction). These equations indicate that the mixed states can display a very fast decay (of the order of τ_C) that can be significantly shorter than the bare exciton decay time.

The photon lifetime in the cavity τ_C is given by[28]

$$\tau_C = \frac{2nL_c m_{\rm eff}}{(1-R_1R_2)c} = \frac{m_{\rm eff}F\hbar}{E}, \qquad (10)$$

where R_1 and R_2 are the reflection coefficients of the two cavity mirrors and F is the finesse of the cavity far from resonance. We have calculated the finesse through a transfer-matrix model applied to the whole structure, with the two Bragg mirrors and without taking into account the exciton resonance. We find $F=442$, $m_{\rm eff}F=2790$, which corresponds to a cavity lifetime equal to 1.3 ps.

Equations (8) and (9) suppose that the wave vector in the plane $k_{\|}$ is conserved. This is not exactly true because the quantum-well interfaces are rough. The position of the in-plane wave vector ($k_{\|}$) is undefined inside a domain limited by $k_{\mathrm{rough}} \sim 1/L_{\mathrm{rough}}$, where L_{rough} is the dimension of the plateaus in the quantum-well interfaces. The true decay rate is then an average of $1/\tau_L$ for $k_{\|} < k_{\mathrm{rough}}$. For simplicity, we suppose that there is a value of $k_{\|}$ (k_{av}) such that $1/\tau_L$ calculated for k_{av} is equal to the average of $1/\tau_L$ in the domain $k_{\|} < k_{\mathrm{rough}}$.

Figure 5 presents a fit of Eq. (9) to our experimental results for the fast decay component of the lower state under resonant excitation with the phenomelogical values $\tau_X = 26$ ps and $k_{\mathrm{av}} = 1.9 \times 10^4$ cm^{-1}. As shown in Fig. 5, this simple model gives a good qualitative variation of the lifetime of the mixed modes with the detuning.

B. The polariton model

The polariton model can give a physical interpretation of Eqs. (8) and (9). For the sake of simplicity, we shall restrict our discussion to the case of resonant excitation on the lower branch. Once created, polaritons can decay either by escaping the cavity with a rate $1/\tau_z$ or by scattering towards regions in k space where the outgoing polaritons will not be detected, at a rate $1/\tau_a$:

$$\frac{1}{\tau} = \frac{1}{\tau_z} + \frac{1}{\tau_a}. \tag{11}$$

The escape time τ_z can be calculated as for the photon lifetime inside a cavity [Eq. (10)] by taking into account the difference between the speed of light c/n and the polariton velocity $\partial E/\partial(\hbar k_z)$ in the equivalent homogeneous material inside the cavity. The escape time of the polaritons τ_z is then

$$\tau_z = \tau_C \frac{\hbar c}{n \dfrac{\partial E}{\partial k_z}}, \tag{12}$$

where $\partial E/\partial k_z$ is calculated using Eq. (4) or (5). This expression depends on δ_0 and $k_{\|}$ and it can be easily shown that $1/\tau_z$ is identical to the second term on the right-hand side of Eq. (9).

The first term (exciton part) on the right-hand side of Eq. (9) is important only for $\delta_0 > 0$. It is due either to the exciton recombination in the leaky modes (for $k_{\|} > k_{\mathrm{SB}}$, where $k_{\mathrm{SB}} = 6 \times 10^4$ cm^{-1} is the limit of the stop band) or to the scattering towards the reservoir through acoustic-phonon interaction. Let us concentrate on this second mechanism. As a matter of fact, the dispersion curves in Fig. 8 underscore important changes in the exciton dynamics introduced by the cavity, through the variation of the energy of the radiant states ($k_{\|}$ small) relative to that of the reservoir ($k_{\|}$ large). Indeed, since the reservoir is not coupled to light, its energy is unaffected by the cavity and corresponds (for $k_{\|}$ not too large) to that of the exciton in a naked well: E_{x0}. As a consequence, we write

$$\frac{1}{\tau_a} = \frac{1}{\tau_{a0}} - \frac{\delta + \Delta}{2\Delta} \exp\left(\frac{E_l(\delta_0, k_{\|}) - E_{x0}}{k_B T} \right), \tag{13}$$

where τ_{a0} is the scattering time of excitons by phonons at large positive detuning or, in a ''naked well,'' $(\delta + \Delta)/2\Delta$ is the exciton weight of the mixed particle [see Eq. (7)] and the exponential term represents the number of available phonons given by a Boltzmann approximation.

On Fig. 5 we have plotted the curve obtained using Eq. (11) for $k_{\|} = k_{\mathrm{av}}$. The fitting parameters are $\tau_{a0} = 15.6$ ps and $k_{\mathrm{av}} = 1.8 \times 10^4$ cm^{-1}. The agreement is very good, keeping in mind the 3-ps resolution of the streak camera, which explains the discrepancy for the negative detunings. The only difference between the two models comes from the Boltzmann factor in $1/\tau_a$ [Eq. (13)], which does not exists in the exciton part of $1/\tau_L$ [Eq. (9)]. In other words, in the first model, we consider that the lifetime of the excitons is constant, while in the second model, the decay rate of the excitons is only due to the scattering by acoustic phonons out from the domain where they can be detected by our optical system. Though the precision of the experimental lifetimes is not very good (~15%) for the large positive detunings, where the luminescence intensity is weak and the decay curves are perturbed by the scattering of the laser on the surface of the sample, the second model is closer to the experimental values. The calculated curve is very sensitive to the value of k_{av} (a decrease of k_{av} by 10% would shift the curve to the right by 1 meV), which confirms that the cavity polariton is a pertinent concept to describe such experiments and that the in-plane wave vector has to be taken into account. Let us note that k_{av} is larger than the $k_{\|}$ value corresponding to the half aperture of the lens with which we observe the luminescence ($\theta = 11°$, $k_{\|} = 1.3 \times 10^4$ cm^{-1}). Up to now, we cannot say whether this difference is due to the interface roughness of the well or to the fact the sample is not exactly perpendicular to the optical axis.

On the basis of our model, we can also give a qualitative account for the whole dynamics of the polaritons, as it appears on Figs. 1 and 3. When excitation is resonant with excitonlike states (E_l for $\delta_0 \gg 0$ or E_u for $\delta_0 \ll 0$), the radiant and reservoir states are close in energy. Thus we observe a luminescence decay very similar to that of a naked well: with a first rapid decay (recombination or scattering to the reservoir) and a second slower decay (return of excitons from the reservoir).

When excitation is resonant with lower photonlike modes (E_l for $\delta_0 \ll 0$), the polaritons created in the radiant states cannot transfer to the reservoir because its energy is much higher. Thus we do not observe the second decay.

When excitation is resonant with upper photonlike modes (E_u for $\delta_0 \gg 0$), the first decay is very fast since there are available reservoir states at large $k_{\|}$. The intensity associated with the second decay is negligible because the excitons in the reservoir cool rapidly and cannot return to the higher-energy radiant states. However, the excitons in the reservoir can transfer via acoustic phonons toward the lower radiant states, which is what we observe (Fig. 4).

Furthermore, we observe a long rising time (~50 ps)

of the luminescence of the lower states for excitation resonant with the upper states and for large positive detunings [Fig. 4(a)], while the luminescence of the upper states is very short (~10 ps). This is proof that the polaritons do not transfer directly from the upper states to the lower states, but that they transfer via a third kind of states: the reservoir.

Finally, the intensity of the instantaneous luminescence at short times for an excitation resonant with the lower branch tends towards zero for large positive detunings (see Fig. 6). This reflects the fact that τ_z tends to infinity because the polariton velocity in the z direction tends towards zero for positive detunings as can be observed in Fig. 7, when k_z is larger than π/L_c. Indeed the instantaneous luminescence intensity I_L at short times is proportional to the inverse escape time in the z direction τ_z and to the number of photons from the pump that are absorbed in the cavity. This latter quantity is proportional to $P_{\mathrm{ex}}(1-R)$, where P_{ex} is the excitation power and R is the reflection coefficient of the cavity at the same energy. The normalized initial luminescence intensity can thus be written as

$$\frac{I_L}{P_{\mathrm{ex}}} \propto \frac{1}{\tau_z}(1-R). \tag{14}$$

The curves given in Fig. 6 show that the ratio I_L/P_{ex} follows the curve $(1-R)/\tau_z$, where the reflection coefficient is obtained from experimental reflectivity spectra and τ_z is calculated using Eq. (12) with $k_{\|}=0$. This confirms that the escape time of the polaritons τ_z tends to infinity when the detuning is positive and large, even if the overall lifetime τ remains finite.

V. SUMMARY AND CONCLUSIONS

Our experimental results on the spontaneous-emission dynamics of resonantly excited quantum-well excitons embedded in a cavity and displaying the exciton-photon mode splitting show that the spontaneous-emission lifetime depends strongly on the detuning: The effect of the cavity can be understood as a strong coupling between the extended exciton states and the cavity modes so that our experiments access directly mixed exciton-photon modes, that is to say, polaritons. When the lower exciton-photon state is more excitonlike, its lifetime is close to that of bare excitons. By changing the detuning, the mixed state evolves continuously into a more photonlike state, so its lifetime decreases continuously to reach the photon lifetime in the cavity. These lifetime changes can be accounted for either through a full polariton model or through a simplified two-level model.

ACKNOWLEDGMENTS

The authors are grateful to C. Tanguy for a critical reading of the manuscript, to Y. Chen for valuable discussions, and to R. Kuszelewicz for the transfer-matrix calculation. This work was supported in part by a Basic Research Action (Project No. 6934 QUINTEC) and by a Basic Research Working Group (Project No. 7070 PHOTONS) within the European Strategic Program in Information Technology (ESPRIT) of the European Commission.

[1] Y. Yamamoto and R. E. Slusher, Phys. Today **46** (6), 66 (1993); R. E. Slusher and C. Weisbuch, Solid State Commun. **92**, 149 (1994).

[2] H. Yokoyama, K. Niche, T. Anan, H. Yamada, S. D. Brorson, and E. P. Ippen, Appl. Phys. Lett. **57**, 2814 (1990).

[3] H. Yokoyama, K. Nishi, T. Anan, Y. Nambu, S. D. Brorson, E. P. Ippen, and M. Suzuki, Opt. Quantum Electron. **24**, S245 (1992).

[4] R. R. Chance, A. Prock, and R. Silbey, in *Advances in Chemical Physics*, edited by I. Prigogine and S. Rice (Wiley, New York, 1978), Vol. XXXVII, p. 1; D. G. Deppe, C. Lei, C. C. Lin, and D. L. Huffaker, J. Mod. Opt. **41**, 325 (1994).

[5] I. Abram and J. L. Oudar, Phys. Rev. A **51**, 4116 (1995).

[6] C. Weisbuch, M. Nishioka, A. Ishikawa, and Y. Arakawa, Phys. Rev. Lett. **69**, 3314 (1992); R. Houdré, R. P. Stanley, U. Oesterle, M. Ilegems, and C. Weisbuch, Phys. Rev. B **49**, 16 761 (1994).

[7] Y. Yamamoto, F. Matinaga, S. Machida, A. Karlsson, J. Jacobson, G. Björk, and T. Mukai. J. Phys. (France) IV **3**, C5-39 (1993).

[8] I. Abram, S. Iung, R. Kuszelewicz, G. Le Roux, C. Licoppe, J. L. Oudar, E. V. K. Rao, J. I. Bloch, R. Planel, and V. Thierry-Mieg, Appl. Phys. Lett. **65**, 2516 (1994).

[9] T. B. Norris, J. K. Rhee, C. Y. Sung, Y. Arakawa, M. Nishioka, and C. Weisbuch, Phys. Rev. B **50**, 14 663 (1994).

[10] H. Cao, J. Jacobson, G. Bjork, S. Pau, and Y. Yamamoto, Appl. Phys. Lett. **66**, 1107 (1995); J. Jacobson, S. Pau, H. Cao, G. Bjork, and Y. Yamamoto, Phys. Rev. A **51**, 2542 (1995).

[11] S. Haroche, in *Fundamental Systems in Quantum Optics*, 1990 Les Houches Lectures Session LIII, edited by J. Dalibard, J. M. Raimond, and J. Zinn-Justin (Elsevier, Amsterdam, 1992), p. 769.

[12] B. Sermage, S. Long, B. Deveaud, and D. S. Katzer, J. Phys. (France) IV **3**, C5-19 (1993); B. Deveaud, F. Clerot, N. Roy, K. Satzke, B. Sermage, and D. S. Katzer, Phys. Rev. Lett. **67**, 2355 (1991).

[13] A. Vinattieri, J. Shah, T. C. Damen, D. S. Kim, L. N. Pfeiffer, M. Z. Maialle, and L. J. Sham, Phys. Rev. B **50**, 10 868 (1994).

[14] S. Pau, G. Björk, J. Jacobson, H. Cao, and Y. Yamamoto, Phys. Rev. B **51**, 14 437 (1995).

[15] Y. Chen, A. Tredicucci, and F. Bassani, Phys. Rev. B **52**, 1800 (1995).

[16] B. Sermage, Ann. Phys. (Paris) Colloq. **20**, C2-297 (1995).

[17] J. J. Hopfield and D. G. Thomas, Phys. Rev. **132**, 563 (1963).

[18] W. C. Tait and R. L. Weiher, Phys. Rev. **166**, 769 (1968).

[19] R. P. Stanley, R. Houdré, U. Oesterle, M. Gailhanou, and M. Illegems, Appl. Phys. Lett. **65**, 1883 (1994).

[20] Y. Zhu, D. J. Gauthier, S. E. Morin, Q. Wu, H. J. Carmichael, and T. W. Mossberg, Phys. Rev. Lett. **64**, 2499 (1990).

[21] R. Houdré, C. Weisbuch, R. P. Stanley, U. Oesterle, P. Pellandini, and M. Illegems, Phys. Rev. Lett. **73**, 2043 (1994).

[22] H. G. Grimmeis and B. Monemar, Phys. Status Solidi **5**, 109 (1971).
[23] S. R. Kisting, P. W. Bohn, E. Andideh, I. Adesida, B. T. Cunningham, G. E. Stillman, and T. D. Harris, Appl. Phys. Lett. **57**, 1328 (1990).
[24] R. Atanasov, F. Bassani, A. D'Andrea, and N. Tomassini, Phys. Rev. B **50**, 14 381 (1994).
[25] K. J. Moore, G. Duggan, K. Woodbridge, and C. Roberts, Phys. Rev. B **41**, 1090 (1990).
[26] R. G. Ulbrich and C. Weisbuch, Phys. Rev. Lett. **38**, 865 (1977).
[27] W. Ekardt, K. Lösch, and D. Bimberg, Phys. Rev. B **20**, 3303 (1979).
[28] R. Houdré, R. P. Stanley, U. Oesterle, M. Illegems, and C. Weisbuch J. Phys. (France) IV **3** C5-51 (1993).